



King Saud University
Arabian Journal of Chemistry

www.ksu.edu.sa
www.sciencedirect.com



ORIGINAL ARTICLE

Removal of malachite green dye from aqueous solution with adsorption technique using *Limonia acidissima* (wood apple) shell as low cost adsorbent

Ashish S. Sartape^a, Aniruddha M. Mandhare^a, Vikas V. Jadhav^b,
Prakash D. Raut^b, Mansing A. Anuse^a, Sanjay S. Kolekar^{a,*}

^a Analytical Chemistry Laboratory, Department of Chemistry, Shivaji University, Kolhapur 416 004, India

^b Department of Environmental Science, Shivaji University, Kolhapur 416 004, India

Received 26 September 2012; accepted 22 December 2013

KEYWORDS

Wood apple shell;
Biosorption;
Adsorption isotherm;
Kinetic study;
FTIR study

Abstract In the present study, the use of low-cost, abundantly available, highly efficient and eco-friendly adsorbent wood apple shell (WAS) has been reported as an alternative to the current expensive methods of removing of malachite green (MG) dye from aqueous solution. The effects of different variables, adsorbent dosage, initial dye concentration, pH, contact time, temperature etc. were investigated and optimal experimental conditions were ascertained. The Langmuir isotherm model has given a better conformity than the Freundlich model with 80.645 mg/g as maximum adsorption capacity at 299 K. The adsorption of MG on WAS was confirmed by FTIR, SEM study, as it showed the change in characterization before and after adsorption. It was found that the Lagergren's model could be used for the prediction of the system's kinetics, while intraparticle diffusion study and Boyd plot were used to furnish the mechanistic study. Thermodynamic study concluded the spontaneous and endothermic nature of the adsorption. Present investigation and comparison with other reported adsorbents concluded that, WAS may be applied as a low-cost attractive option for removal of MG from aqueous solution.

© 2013 King Saud University. Production and hosting by Elsevier B.V. All rights reserved.

1. Introduction

Dyes are used in large quantities in many industries including textile, leather, cosmetics, paper, printing, plastic, pharmaceuticals, food, etc. to colour their products, which generates wastewater, characteristically high in colour and organic content. The textile industry alone accounts for two third of the total dye stuff production (Azhar et al., 2005; Garg et al., 2004). The discharge of coloured wastes into streams not only affects their aesthetic nature but also interferes with the

* Corresponding author. Tel.: +91 9881762426; fax: +91 2312692333.

E-mail addresses: sartape_chem@yahoo.co.in (A.S. Sartape), kolekarss2003@yahoo.co.in (S.S. Kolekar).

Peer review under responsibility of King Saud University.



Production and hosting by Elsevier

Nomenclature

| | | | |
|------------------|---|------------------|--|
| b_f | Freundlich isotherm exponent | k_1 | pseudo first order rate constants for adsorption |
| Bt | mathematical function of F | k_2 | pseudo second order rate constant (g/mg min) |
| c | constant | M | weight of adsorbent (g) |
| C_e | equilibrium concentration (mg/L) of MG dye | q_e | amount adsorbed on adsorbent (mg/g) |
| C_0 | initial concentration (mg/L) of MG dye | q_m | Langmuir monolayer adsorption capacity (mg/g) |
| D_i | diffusion coefficient (cm ² /s) | q_t | amount adsorbed at time t (mg/g) |
| F | the fraction of solute adsorbed at any time | R_L | dimensionless equilibrium parameter |
| ΔG° | standard Gibbs energy of adsorption (kJ/mol) | R^2 | correlation coefficient |
| ΔH° | standard enthalpy of adsorption (kJ/mol) | ΔS° | standard entropy of adsorption (J/mol K) |
| K_c | equilibrium constant | T | temperature (K) |
| K_f | Freundlich multilayer adsorption capacity (mg/g) | t | time (min) |
| k_{id} | intraparticle diffusion rate (mg/g min ^{1/2}) | V | volume (L) of the solution |
| K_L | Langmuir equilibrium constant of adsorption (L/mg) | | |

transmission of sunlight into streams and therefore reduces photosynthetic action. Further, coloured wastes may contain chemicals which exhibit toxic effects towards microbial populations and can be toxic and/or carcinogenic to mammals. In general, dyes are poorly biodegradable. Conventional biological treatment processes are not very effective in dye removal (Ashtouky El, 2009). Basic malachite green (MG) dye has been widely used for the dyeing of leather, wool, jute and silk, as in distilleries, as a fungicide and antiseptic in aquaculture industry to control fish parasites and disease (Zhang et al., 2008). Malachite green has properties that make it difficult to remove from aqueous solutions and also toxic to major microorganisms. Though, the use of this dye has been banned in several countries and not approved by US Food and Drug Administration, it is still being used in many parts of the world due to its low cost, easy availability and efficacy and to lack of a proper alternative (Hameed and El-Khaiary, 2008a; Papinutti et al., 2006).

Malachite green is environmentally persistent and acutely toxic to a wide range of aquatic and terrestrial animals. It is highly lethal to freshwater fish, in both acute and chronic exposures. It causes serious public health hazards and also poses potential environmental problem. Both clinical and experimental observations reported so far reveal that MG is a multi-organ toxin. It decreases food intake, growth and fertility rates; causes damage to the liver, spleen, kidney and heart; inflicts lesions on the skin, eyes, lungs and bones; and produces teratogenic effects. Malachite green is highly cytotoxic to mammalian cells. Incidences of tumour in the lungs, breast and ovary have also been reported from rats exposed to MG. It also acts as a respiratory enzyme poison. Decrease in RBC count (dyscrasia), Hb (anaemia) and HTC (%); increase in WBC count (leukocytosis) and delay in blood coagulation were observed post-exposure to MG (Srivastav et al., 1999; Srivastava et al., 2004; Yonar and Yonar, 2010).

Possible methods of dye removal from textile effluents include chemical oxidation, froth flotation, adsorption, coagulation, electro-dialysis, cloud point extraction etc. (Elhami, 2010; Gupta et al., 1997). Amongst these, the adsorption methods currently appear to offer the best potential for overall treatment, and it could be expected to be promising for a wide range of compounds, than any of the other listed processes.

Recognizing the high cost of activated carbon, many investigators have studied the feasibility of economical, commercially available materials as its possible replacements. Biosorption based on binding capacities of different low-cost adsorbents includes natural, agricultural, and industrial by-product wastes. They are attractive because of their abundant availability at low or no cost, their good performance in removing dyes from aqueous solutions as well as minimum volume of sludge to be disposed (Hameed and El-Khaiary, 2008b; Saha et al., 2010). Previously several researchers had proved several low cost materials such as, wheat bran (Papinutti et al., 2006), tamarind fruit shell (Saha et al., 2010), marine alga *Caulerpa racemosa* var. *cylindracea* (Bekci et al., 2009), hen feathers (Mittal, 2006), pithophora species fresh water algae (Kumar et al., 2006) etc.

In the present study, wood apple shell (WAS) has been used as adsorbent whose results showed good capacity of adsorption of MG in very short period of agitation. The *Limonia acidissima* (wood apple) is used medicinally as well as in making of sweet in India. Unemployed shell of fruit is waste which became the best application as the effective and inexpensive adsorbent. The study was carried out with isotherm as well as kinetic models, along with the thermodynamic study.

2. Materials and methods

2.1. Preparation of adsorbent and dye solution

The wood apple shells were collected from local market and washed repeatedly with distilled water to remove dust and soluble impurity. These were dried in shadow at room temperature and then crushed in mechanical grinder. Once again it was washed to remove colouring matter of adsorbent and followed by drying in oven at 383 K for 24 h. The dried material was then passed through the BSS 44 sieves after which it became ready for use as adsorbent. Adsorption behaviour depends on the method of preparation and the prior treatment of the adsorbent. The adsorbent sample once prepared was stored and used throughout the series.

The MG dye has molecular formula $C_{23}H_{25}N_2Cl$ (molecular weight = 364.92, λ_{max} = 615 nm) (Fig. 1). Stock solution of 1000 mg/L was prepared with double distilled water.

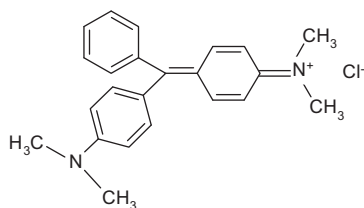


Figure 1 Structural formula of malachite green dye.

All working solutions used in tests were prepared by appropriately diluting the stock solution to a pre-determined concentration. All other chemicals used in this study were analytical reagent grade.

2.2. Characterization of adsorbent

The adsorbent, WAS, was characterized with Fourier Transform Infra Red Spectroscopy (FTIR) (Perkin Elmer, Spectrum 100) and Scanning Electron Microscopy (SEM) (JEOL, JSM-360). The elemental analysis was carried out with Elemental analyser (EA 1108, Carlo Erba). The other properties such as moisture, ash content, etc. were determined as listed in Table 1.

The FTIR spectrum of the WAS (Fig. 2) has shown the various functional groups with respect to their peak value. Peak at 3406 and 2925 cm^{-1} indicates the functional group OH and C-H, respectively. The peak values at 1738, 1634, 1249, and 1041 cm^{-1} confirm the functional groups C=O stretch, C=C, C-C, C-H bending, respectively. The surface morphology was characterized with SEM, before and after adsorption (Figs. 4 and 5) of MG on WAS, respectively.

2.3. Batch adsorption experiment

The experiment was carried out by the batch adsorption method in the Erlenmeyer flasks agitated at 299 ± 2 K for a pre-determined period with isothermal orbital shaker. The adsorption parameters such as pH, time, initial dye concentration, rpm, and temperature were studied. The isotherm study was carried out with different initial concentrations of MG from 100 to 700 mg/L, by keeping temperature constant and at 150 rpm agitation speed for 3.30 h. The adsorbent dosages were checked from 0.05 to 0.4 g/L for better adsorption. The kinetic study was done by varying time from 0 to 210 min. For the thermodynamic study temperature was varied from 303 to 323 K. The measurement of absorbance of colour was

Table 1 Characteristics of wood apple shell activated carbon.

| Property | Result |
|------------------|-------------------------|
| Ash content | 5.21% |
| Bulk density | 0.634 g/cm ³ |
| Moisture content | 3.36% |
| Carbon | 51.62% |
| Hydrogen | 7.16% |
| Nitrogen | 0.12% |

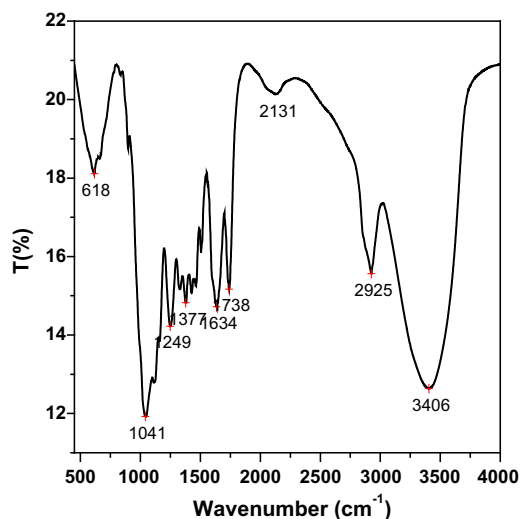


Figure 2 FTIR spectrum of wood apple shell powder.

done spectrophotometrically (Elico, SL 171) at $\lambda_{\text{max}} = 615$ nm. The equilibrium adsorption capacity was evaluated using the equation,

$$q_e = (C_0 - C_e)V/M \quad (1)$$

where q_e (mg/g) is the equilibrium adsorption capacity, C_0 and C_e are the initial and equilibrium concentrations (mg/L) of MG dye solution, V is the volume and M is the weight of adsorbent.

3. Results and discussion

3.1. Analysis of adsorbent

The structure of MG gives the direction for possible functional groups observed on MG dye adsorbed on WAS surface. The major peaks are observed in region 450–1800 cm^{-1} (Fig. 3). The FTIR spectrum of WAS shows peaks at 1738, 1634,

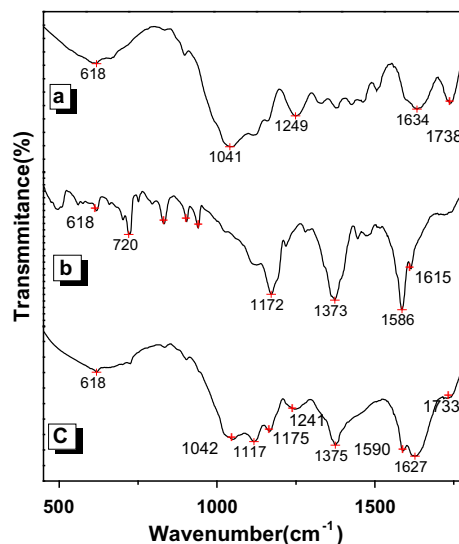


Figure 3 FTIR spectrum of (a) wood apple (b) MG dye (c) MG dye adsorbed on WAS.

1249, 1041 cm^{-1} (Fig. 3(a)), whereas in case of the MG the peaks were recorded at 1615, 1586, 1373, 1172 cm^{-1} (Fig. 3(b)). The peak at 1615 and 1586 cm^{-1} corresponds to C=C aromatic stretching and peak at 1373 cm^{-1} was due to C-C aromatic stretching while 1172 cm^{-1} was due to C-N stretching. Fig. 3(c) shows the FTIR spectrum of MG dye adsorbed on WAS, where the peaks were slightly shifted towards higher side with values 1733, 1627, 1241, 1042 cm^{-1} . This shift in peak values may be due to the formation of chemical bond between functional groups present on WAS and MG; the same observations are reported (Al-Ghouti et al., 2003; Bekci et al., 2009; Sekhar et al., 2009). On the basis of the FTIR one can confirm the adsorption of dye on WAS.

SEM characterization of WAS, before and after adsorption, showed complete change in surface texture. Before adsorption there was the rough surface morphology as observed (Fig. 4), while after adsorption of dye on the WAS, layer on the surface of adsorbent and smoother morphology was observed (Fig. 5). These changes in the morphologies are in good agreement with the literature for various materials (Al-Ghouti et al., 2003; Santhi et al., 2010a; Saha et al., 2010).

3.2. Effect of pH

Initial pH of dye can influence the adsorption of it on the surface of adsorbent. In the present study, pH 1–10 was used to

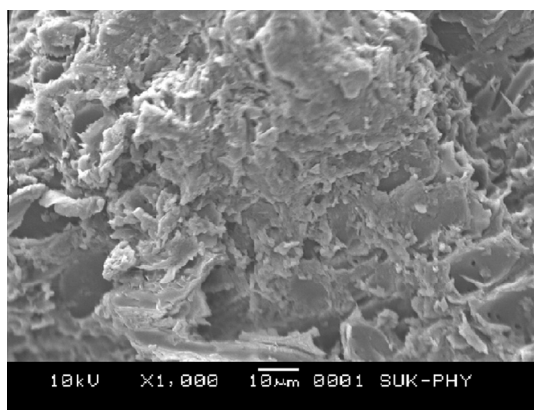


Figure 4 SEM image of WAS before adsorption of MG dye.

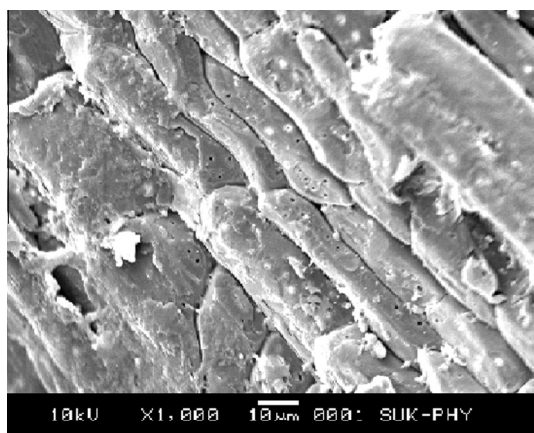


Figure 5 SEM image of WAS after adsorption of MG dye.

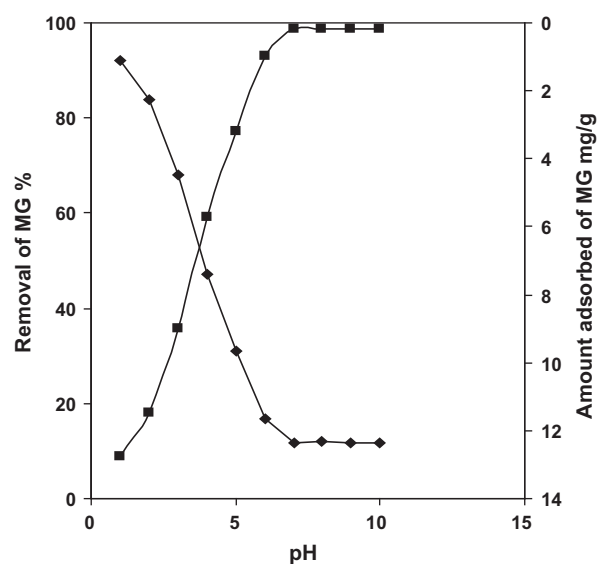


Figure 6 Effect of pH on percentage removal of MG and amount adsorbed mg/g.

observe the better adsorption with initial concentration of dye 100 mg/L with 400 mg WAS as adsorbent dosage. The reaction mixture was agitated for 3.30 h with agitating speed 150 rpm at 299 ± 2 K. The most favourable adsorption was seen at basic pH 7–9 with 98.87% removal of MG dye (Fig. 6). It is well known that from pH 10.50 and more the colour of the dye was self fed. It may be due to the formation of the new species of dye, so for further study pH 7.5–8 was maintained.

At lower pH, the number of positively charged adsorbent surface sites increased at the expense of the number of negatively charged surface sites. The carboxylic groups of MG ($pK_a = 10.3$) were protonated and had high positive charge density at a lower pH (Garg et al., 2003). Consequently, electrostatic repulsion between the positively charged surface and the positively charged dye molecule increased with increasing solution pH and resulting in the decrease of adsorption capacity of MG to the adsorbent. In addition, the competition of H^+ ion with the cationic dye molecules also decreased the adsorption. On the contrary, the functional groups as hydroxyl and carbonyl can act as biosorbing agents or sites with negative charges. The surface of the adsorbent was negatively charged at higher pH, which favoured for adsorption of the positively charged dye cations through electrostatic force of attraction. The adsorption of MG to adsorbent consequently increased with an increase of pH values (Pan and Zhang, 2009; Baek et al., 2010).

3.3. Effect of time

The percentage of dye removal as a function of time was studied, with an initial 100 mg/L concentration of MG dye and adsorbent dosage of 400 mg. The uptake of dye by WAS adsorbent occurs at a faster rate, corresponding to 98.87% removal at an equilibrium time of 210 min (3.30 h). There was faster rate of adsorption at initial stage which went on decreasing later; it may be due to availability of complete active bare surface. The relative increase in the removal of

dye after contact time of 3.30 h was not significant and hence it was fixed as the optimum contact time. The present findings were in good agreement with the earlier reports (Basar et al., 2005; Kannan and Sundaram, 2001). In batch type adsorption systems, a monolayer of adsorbate is normally formed on the surface of the adsorbent, and the rate of removal of adsorbate species from aqueous solution is controlled primarily by the rate of transport of the adsorbate species from the exterior/outer sites to the interior site of the adsorbent particles (Malik et al., 2007).

3.4. Effect of initial concentration

The influence of the initial concentration of MG in the solution on the rate of adsorption on WAS was investigated. The experiment was carried out with fixed adsorbent dosage, along with stably maintained temperature, at basic pH condition. The percent adsorption decreased with an increase in initial dye concentration. The adsorption capacity for WAS was increased from 12.35 to 80.645 mg/g as the MG concentration in the test solution was increased from 100 to 700 mg/L. Maximum dye was sequestered from the solution within 3.30 h after the start of every experiment. WAS took about 3.30 h for equilibrium attainment. Increase in concentration enhances the interaction between the dye and adsorbent apart from providing necessary driving force to overcome the resistances to mass transfer of dye. Therefore, rate of adsorption and hence dye uptake increased with an increase in dye concentration.

3.5. Effect of adsorbent dosage and agitation speed

The percent adsorption and amount adsorbed were increased as the adsorbent doses were increased from 0.05 to 0.4 g at 100 mg/L dye concentration on equilibrium time of 3.30 h. There was 98.87% removal of MG dye with 12.35 mg/g amount adsorbed was observed. From Fig. 7 it is readily understood that the number of available adsorption sites and the surface area increase by increasing the adsorbent dose, it therefore, results in the increase of amount of adsorbed dye.

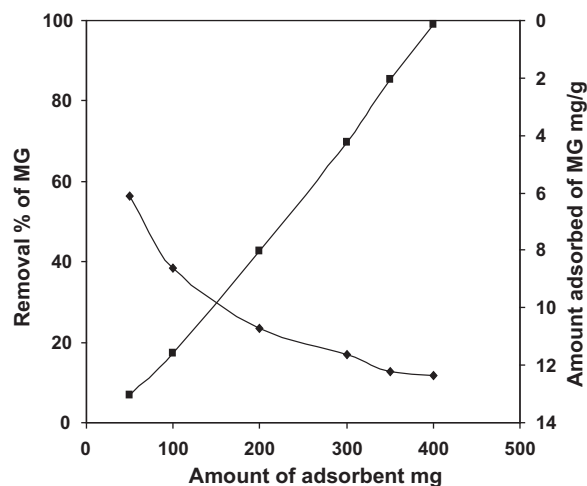


Figure 7 Effect of adsorbent dosage on percentage removal and amount adsorbed mg/g of MG.

After formation of equilibrium, it was observed a decrease in amount of adsorption. This may be attributed to overlapping or aggregation of adsorption sites resulting in a decrease in total adsorbent surface area available to MG and as an increase in diffusion path length (Garg et al., 2004).

The agitating speed was varied from 50 to 250 rpm, but from 150 rpm the results did not show any disparity, it remains invariable with amount adsorbed as well as percent removal of MG. For both the experiments the dye concentration was maintained at 100 mg/L, while time, temperature and all parameters were kept constant.

3.6. Adsorption isotherm

In order to optimize the design of an adsorption system to remove the dye, it is important to establish the most appropriate correlations of the equilibrium data of each system. Equilibrium isotherm equations are used to describe the experimental adsorption data. The parameters obtained from the different models provide important information on the adsorption mechanisms and the surface properties and affinities of the adsorbent.

The most widely accepted surface adsorption models for single-solute systems are the Langmuir and Freundlich models. The correlation with the amount of adsorption and the liquid-phase concentration was tested with them. Linear regression is frequently used to determine the best-fitting isotherm, and the applicability of isotherm equations is compared by judging the correlation coefficients.

3.7. Langmuir isotherm

The theoretical Langmuir isotherm is valid for adsorption of a solute from a liquid solution as monolayer adsorption on a surface containing a finite number of identical sites. Langmuir isotherm model assumes uniform energies of adsorption onto the surface without transmigration of adsorbate in the plane of the surface (Santhi et al., 2010a). Therefore, the Langmuir isotherm model was chosen for the estimation of the maximum adsorption capacity corresponding to complete monolayer coverage on the adsorbent surface. The Langmuir equation (Saha et al., 2010) is commonly expressed as follows:

$$C_e/q_e = (1/K_L q_m) + (1/q_m)C_e \quad (2)$$

where q_m is monolayer adsorption capacity (mg/g), K_L is Langmuir isotherm constant related to the affinity of the binding sites and energy of adsorption (L/mg). The values of q_m and K_L can be calculated by plotting C_e/q_e versus C_e (Fig. 8). The essential characteristics of a Langmuir isotherm can be expressed in terms of a dimensionless constant separation factor or equilibrium parameter, R_L (Hall et al., 1966), which is defined by

$$R_L = 1/(1 + K_L C_e) \quad (3)$$

The influence of isotherm shape on “favourable” or “unfavourable” adsorption has been considered (Gupta et al., 1997). The R_L values indicate the type of the isotherm to be either unfavourable ($R_L > 1$), linear ($R_L = 1$), favourable ($0 < R_L < 1$) or irreversible ($R_L = 0$). In the present experiment the results were found for R_L between 0.7386 and 0.0465 which clearly indicate the adsorption was favourable.

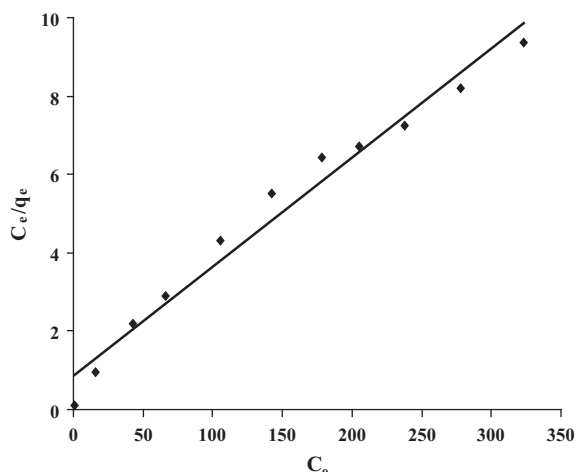


Figure 8 Langmuir isotherm for MG adsorption on WAS.

Fig. 8 shows the plot of C_e/q_e versus C_e for the adsorption of MG onto WAS at constant temperature according to the linear forms of Langmuir isotherm.

3.8. Freundlich Isotherm

The Freundlich equation was employed for the adsorption of MG dye on the adsorbent. The Freundlich isotherm (Hema and Arivoli, 2008) was represented by

$$\log q_e = \log K_f + 1/n \log C_e \quad (4)$$

where q_e is the amount of MG dye adsorbed (mg/g), C_e is the equilibrium concentration of dye in solution (mg/L), and K_f and n are constants incorporating the factors affecting the adsorption capacity and intensity of adsorption, respectively. Linear plots of $\log q_e$ versus $\log C_e$ (Fig. 9) shows that the adsorption of MG dye obeys the Freundlich adsorption isotherm. The values of K_f and n given in Table 2 show that the increase of negative charges on the adsorbent surface makes electrostatic force like van der Waals force between the surface and dye. The molecular weight and size either limit or increase

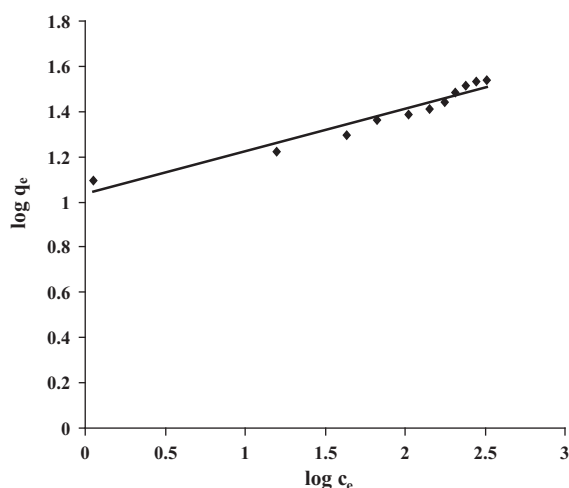


Figure 9 Freundlich isotherm for adsorption of MG on WAS.

Table 2 Langmuir and Freundlich constant for the adsorption of MG on WAS.

| Langmuir constants | | | Freundlich constants | | |
|--------------------|--------------|-------|----------------------|------|-------|
| q_m (mg/g) | K_L (L/mg) | R^2 | K_f | n | R^2 |
| 35.84 | 0.033 | 0.974 | 10.81 | 5.32 | 0.941 |

the possibility of the adsorption of the dye onto adsorbent. However, the values clearly show the dominance in adsorption capacity. The intensity of adsorption is an indication of the bond energies between dye and adsorbent, and the possibility of slight chemisorptions rather than physisorption (Arivoli et al., 2009).

The results indicate that there is better fitting of Langmuir isotherm model than the Freundlich isotherm (Table 2). On this basis also one could conclude that, it was chemisorption.

3.9. Kinetic study of adsorption

The kinetics of MG dye adsorption onto WAS is required for selecting optimum operating conditions for the full-scale batch process. The kinetic parameters, which are helpful for the prediction of adsorption rate, give important information for designing and modelling the adsorption processes (Santhi et al., 2010b). In order to investigate the mechanism of adsorption various kinetic models have been suggested. In recent years, adsorption mechanisms involving kinetics-based models have been reported. In this study, two of the well known models were investigated to find the best fitted model for the experimental data obtained.

The kinetic data were treated with the following Lagergren's pseudo first-order rate equation (Ho and McKay, 1999).

$$\log(q_e - q_t) = \log q_e - k_1 t / 2.303 \quad (5)$$

where q_t and q_e are the amount adsorbed at time t and at equilibrium (mg/g) and k_1 is the pseudo first-order rate constant for the adsorption process (min^{-1}). The pseudo second-order model can be represented in the following form (Ho and McKay, 1998; Zhang et al., 2008).

$$t/q_t = 1/k_2 q_e^2 + t/q_e \quad (6)$$

where k_2 is the pseudo second order rate constant (g/mg min). The plots of $\log(q_e - q_t)$ versus t and the plots of t/q_t versus t are shown in Figs. 10 and 11, respectively. Kinetic constants calculated from slope and intercept of plots for both the models are given in Table 3 which shows that pseudo first-order is better fitted than pseudo second-order.

3.10. Mechanistic study

If the intraparticle diffusion is involved in the adsorption processes, then the plot of the square root of time versus the uptake (q_t) would result in a linear relationship and the intraparticle diffusion would be the controlling step if this line passed through the origin. When the plots do not pass through the origin, this is indicative of some degree of boundary layer control and this further shows that the intraparticle diffusion is not the only rate controlling step, but also other processes may control the rate of adsorption (Alzaydien, 2009). In order to

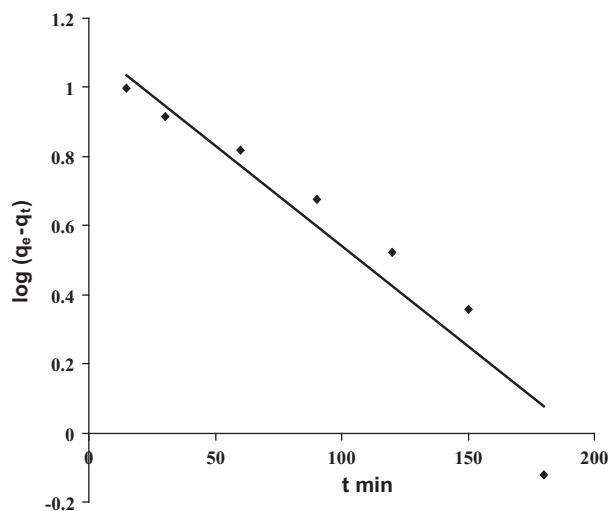


Figure 10 Pseudo first-order reaction of adsorption of MG on WAS.

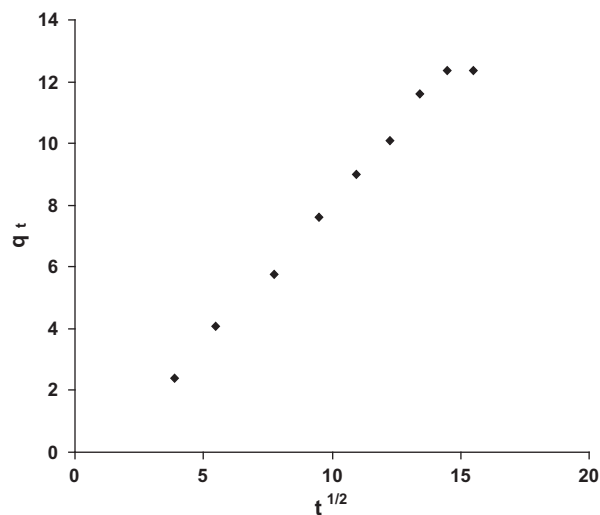


Figure 12 Intraparticle diffusion plot for adsorption of MG on WAS.

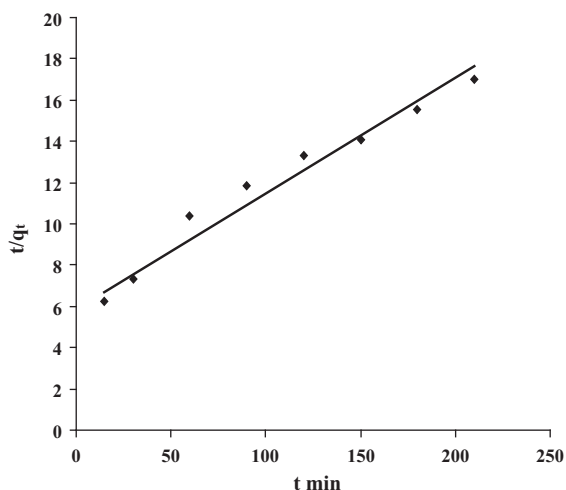


Figure 11 Pseudo second-order reaction of adsorption of MG on WAS.

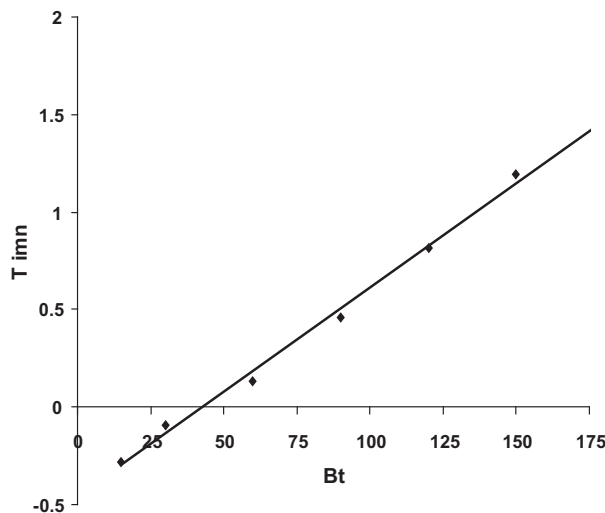


Figure 13 Boyd plot of adsorption of MG on WAS.

investigate the mechanism of the MG adsorption onto WAS, intraparticle diffusion based mechanism was studied. The most commonly used technique for identifying the mechanism involved in the adsorption process is by fitting an intraparticle diffusion plot. It is an empirically found functional relationship, common to the most adsorption processes, where uptake varies almost proportionally with $t^{1/2}$ rather than with the contact time t (El-Latif et al., 2010).

$$q_t = k_{id}t^{1/2} + c \quad (7)$$

where, c is constant and k_{id} is the intraparticle diffusion rate constant ($\text{mg/g min}^{1/2}$), q_t is the amount adsorbed (mg/g) at a time t (min). The intraparticle diffusion rate constant was determined from the slope of the linear gradients of the plot q_t versus $t^{1/2}$ (Fig. 12).

From a mechanistic viewpoint to interpret the experimental data, it is necessary to identify the steps involved during adsorption described by external mass transfer (boundary layer diffusion) and intraparticle diffusion. From design aspect, it is important to estimate which is the rate-limiting step (pore or

Table 3 Kinetic parameters for the effect of temperature on the removal of MG.

| Pseudo first-order | | | | Pseudo second-order | | | Intraparticle diffusion | | Boyd diffusion coefficient |
|--------------------|--|--------------------|-------|--|--------------------|-------|--------------------------------------|-------|---|
| q_e exp. (mg/g) | $k_1 \times 10^{-3}$ (min^{-1}) | q_e calc. (mg/g) | R^2 | $k_2 \times 10^{-3}$ (mg/g min) | q_e calc. (mg/g) | R^2 | K_{id} ($\text{mg/g min}^{1/2}$) | R^2 | $D_i \times 10^{-5}$ (cm^2/s) |
| 12.35 | 0.58 | 13.23 | 0.92 | 53.52 | 17.86 | 0.96 | 0.825 | 0.98 | 2.07 |

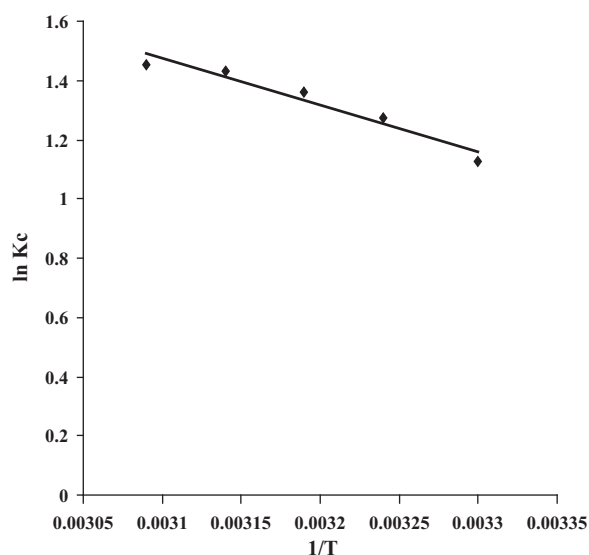


Figure 14 Van't Hoff plots for adsorption of MG on WAS.

Table 4 Thermodynamic parameters of WAS.

| T (K) | ΔG° (kJ/mol) | ΔH° (kJ/mol) | ΔS° (J/mol K) |
|---------|---------------------------|---------------------------|----------------------------|
| 303 | -2.832 | 1.581 | 6.375 |
| 308 | -3.268 | | |
| 313 | -3.547 | | |
| 318 | -3.781 | | |
| 323 | -3.907 | | |

surface diffusion) involved in the sorption process (Kumaretal., 2006). Thus kinetic data have been analysed using the model given by Boyd et al. (1947).

$$F = 1 - (6/\pi^2) \exp(-Bt) \quad (8)$$

and

$$F = q/q_e \quad (9)$$

where q_e is the amount of malachite green adsorbed at equilibrium time (mg/g) and q represents the amount of dye adsorbed at any time t (min), F represents the fraction of solute adsorbed at any time t and Bt is a mathematical function of F .

Substituting Eq. (9) in Eq. (8), Eq. (8) simplifies to

$$1 - F = (6/\pi^2) \exp(-Bt) \quad (10)$$

or

$$Bt = -0.4977 - \ln(1 - F) \quad (11)$$

Eq. (11) is used to calculate Bt values at different time t . The calculated Bt values were plotted against time as shown in Fig. 13. The linearity in the plot is used to distinguish whether external and intraparticle transport controls the adsorption rate. From Fig. 13 it was observed that the relation between Bt and t was linear at all dye concentrations but does not pass through origin, confirming that surface diffusion is the rate-limiting step. The calculated Bt values were used to calculate the effective diffusion coefficient, D_i (cm^2/s) using the relation (Kumar et al., 2006).

$$B = \pi^2 D_i / r^2 \quad (12)$$

where, r represents the radius of the particle calculated by sieve analysis and by assuming as spherical particles. The average D_i values were estimated to be $2.0659 \times 10^{-5} \text{ cm}^2/\text{s}$. The rate constant of intraparticle diffusion and value of diffusion coefficient D_i are given in Table 3.

Table 5 Comparison of adsorption capacity of WAS with other adsorbent to adsorb MG.

| Adsorbent | Capacity (mg/g) | Condition | | References |
|--|-----------------|-----------|-----------|---------------------------------------|
| | | pH | Temp. (K) | |
| Carbon prepared from <i>Borassus</i> bark | 20.70 | 6 | 303 | Arivoli et al. (2009) |
| <i>Caulerpa racemosa</i> var. <i>cylindracea</i> (marine alga) | 25.67 | 6 | 318 | Bekci et al. (2009) |
| <i>Saccharomyces cerevisiae</i> | 17 | 5 | 308 | Godbole and Sawant (2006) |
| Potato peel | 32.39 | 4 | 298 | Guechi and Hamdaoui (2011) |
| Leaves of <i>Solanum tuberosum</i> | 33.3 | 7 | 303 | Gupta et al. (2011) |
| Stem of <i>Solanum tuberosum</i> | 27 | | | |
| Unsaturated polyester Ce(IV) phosphate | 1.01 | 8 | 300 | Khan et al. (2010) |
| Neem sawdust | 4.35 | 7.2 | 303 | Khattri and Singh (2009) |
| Rubber wood sawdust | 36.45 | - | 305 | Kumar and Sivanesan (2007) |
| Commercial activated carbon | 8.27 | 7 | 303 | Mall et al. (2005) |
| Waste fruit residues | 37.03 | 5-8 | 300 | Parimaladevi and Venkateswaran (2011) |
| Dried cashew nut bark carbon | 20.09 | 6.60 | | Parthasarathy et al. (2011) |
| Tamarind fruit shell | 1.95 | 5 | 303 | Saha et al. (2010) |
| Epicarp of <i>Ricinus communis</i> activated carbon | 27.78 | | | Santhi et al. (2010a) |
| <i>Annona squamosa</i> seed activated carbon | 25.91 | 7 | 300 | Santhi et al. (2010b) |
| <i>Annona squamosa</i> seed | 25.91 | 6 | 300 | Santhi et al. (2011) |
| Cellulose powder | 2.422 | 7.2 | 298 | Sekhar et al. (2009) |
| Kapok hull activated carbon | 30.16 | 6.7 | 300 | Syed (2011) |
| Chlorella-based biomass | 18.4 | 7 | 298 | Tsai and Chen (2010) |
| Carbon prepared from <i>Arundo donax</i> root | 8.69 | 5-7 | 303 | Zhang et al. (2008) |
| Wood apple shell | 34.56 | 7.5 | 299 | Present study |

3.11. Effect of temperature

The adsorption process is temperature dependant. As the temperature rises the capacity of the adsorbent enhances. In the present experiment the temperature study was done from 303 to 323 K with variation of 5 K. The amount of adsorption was increased from 80.55 to 85.31 mg/g with respect to temperature. For temperature study the initial concentration was maintained at 700 mg/L and all other conditions like volume of solution, agitation time, adsorbent dose etc. were kept constant.

Where the temperature is concerned for sorption, it is useful to determine the thermodynamic parameters such as standard Gibbs free energy change ΔG° , standard enthalpy change ΔH° , and standard entropy change ΔS° . The Gibbs free energy change for sorption of MG onto WAS is estimated by using equilibrium constant K_c and can be written as

$$\Delta G^\circ = -RT \ln K_c \quad (13)$$

Standard enthalpy change and standard entropy change ΔS° of adsorption were calculated from van't Hoff equation with the following relation.

$$\ln K_c = \Delta S^\circ / R - \Delta H^\circ / RT \quad (14)$$

where K_c is equilibrium constant for sorption, R gas constant, T temperature (K). The value of ΔH° was calculated from the slope of the linear regression of $\ln K_c$ versus $1/T$ (Fig. 14). The K_c value was determined by the relation given below

$$K_c = q_e / C_e \quad (15)$$

where q_e represents the amount of MG adsorbed on WAS at equilibrium (mg/L), C_e the equilibrium concentration of MG in solution (mg/L). Table 4 illustrates the thermodynamic parameters that were calculated by above equations. The absolute magnitude of ΔG° gives an idea about the type of adsorption. The spontaneous nature of sorption appears due to negative values of ΔG° and average value was found -4.933 kJ/mol. This confirms affinity of WAS for the MG. The positive ΔH° values could lead to endothermic nature of interaction between MG dye and WAS adsorbent. Standard entropy determines the disorderliness of the adsorption at solid-liquid interface.

4. Comparison with other adsorbents

In comparison with the other adsorbents for MG removal, the present study takes places in short time and at room temperature (Table 5). On this basis, one could conclude that, WAS is the economical, efficient and effective adsorbent as compared with reported adsorbents.

5. Conclusion

Wood apple shell, a fruit-food solid waste, was successfully utilized as a low cost alternative adsorbent for the removal of hazardous dye MG. The removal of MG dye was found to be 98.87% with initial concentration 100 mg/L at pH 7–9 in 3.30 h by shaking at 150 rpm at 299 ± 2 K. The shifting of peaks in FTIR spectrum confirmed the MG dye adsorption onto WAS. The SEM study also made support to it by observing difference in surface morphology of adsorbent before and

after adsorption of MG. The adsorption equilibrium data showed good fit to the Langmuir isotherm model as compared to the Freundlich isotherm model. The adsorption kinetics followed pseudo first-order kinetic equation for sorption of MG onto WAS. Thermodynamic study demonstrates the spontaneous and endothermic nature of biosorption process due to negative values of free energy change and positive value of enthalpy change, respectively. Finally it is concluded that, the present adsorbent could be a good alternative for the removal of MG from aqueous solution very effectively and economically.

Acknowledgments

The authors acknowledge Dr. V. M. Gurame, Department of Chemistry, Shivaji University, Kolhapur.

The authors acknowledge the DST-FIST and UGC-SAP facilities of Department of Chemistry, Shivaji University, Kolhapur.

References

- Al-Ghouti, M.A., Khraisheh, M.A.M., Allen, S.J., Ahmad, M.N., 2003. The removal of dyes from textile wastewater: a study of the physical characteristics and adsorption mechanisms of diatomaceous earth. *J. Environ. Manag.* 69, 229.
- Alzaydien, A.S., 2009. Adsorption of methylene blue from aqueous solution onto a low cost natural Jordanian Tripoli. *Am. J. Environ. Sci.* 5 (3), 197.
- Arivoli, S., Hema, M., Martin, P., Prasath, D., 2009. Adsorption of malachite green onto carbon prepared from borassus bark. *Arab. J. Sci. Eng.* 34 (2), 31.
- El Ashtoukhy, S.Z.El., 2009. Loofa egyptiaca as a novel adsorbent for removal of direct blue dye from aqueous solution. *J. Environ. Manag.* 90, 2755.
- Azhar, S.S., Liew, A.G., Suhardy, D., Hafiz, K.F., Hatim, M.D.I., 2005. Dye removal from aqueous solution by using adsorption on treated sugarcane bagasse. *J. Appl. Sci.* 2 (11), 1499.
- Baek, M.H., Ijagbemi, C.O., Jin, O.S., Kim, D.S., 2010. Removal of malachite green from aqueous solution using degreased coffee bean. *J. Hazard. Mater.* 176, 820.
- Basar, C.A., Onal, Y., Kilicer, T., Eren, D., 2005. Adsorptions of high concentration malachite green by two activated carbons having different porous structures. *J. Hazard. Mater. B* 127, 73.
- Bekci, Z., Seki, Y., Cavas, L., 2009. Removal of malachite green by using an invasive marine alga *Caulerpa racemosa* var. *Cylindracea*. *J. Hazard. Mater.* 161, 1454.
- Boyd, G.E., Adamson, A.E., Meyers, L.S., 1947. The exchange of adsorption ions from aqueous solutions by organic zeolites II kinetics. *J. Am. Chem. Soc.* 69, 2836.
- Elhami, N.P.Sh., 2010. Removal of malachite green from water samples by cloud point extraction using Triton X-100 as non-ionic surfactant. *Environ. Chem. Lett.* 8, 53.
- El-Latif, M.M., Ibrahim, A.A., El-Kady, M.M.F., 2010. Adsorption equilibrium, kinetics and thermodynamics of methylene blue from aqueous solutions using biopolymer oak sawdust composite. *J. Am. Sci.* 6 (6), 267.
- Garg, V.K., Gupta, R., Yadav, A.B., Kumar, R., 2003. Dye removal from aqueous solution by adsorption on treated sawdust. *Bioreour. Technol.* 89 (2), 121.
- Garg, V.K., Kumar, R., Gupta, R., 2004. Removal of malachite green dye from aqueous solution by adsorption using agro-industry waste: a case study of *Prosopis cineraria*. *Dyes Pigm.* 62, 1.

- Godbole, P.T., Sawant, A.D., 2006. Removal of malachite green from aqueous solutions using immobilized *Saccharomyces cerevisiae*. *J. Sci. Ind. Res.* 65, 440.
- Guechi, El-K., Hamdaoui, O., 2011. Sorption of malachite green from aqueous solution by potato peel: kinetics and equilibrium modeling using non-linear analysis method. *Arab. J. Chem.* <http://dx.doi.org/10.1016/j.arabjc.2011.05.011>.
- Gupta, N., Kushwaha, A.K., Chattopadhyaya, M.C., 2011. Application of potato (*Solanum tuberosum*) plant wastes for the removal of methylene blue and malachite green dye from aqueous solution. *Arab. J. Chem.* <http://dx.doi.org/10.1016/j.arabjc.2011.07.021>.
- Gupta, V.K., Srivastava, S.K., Mohan, D., 1997. Equilibrium uptake, sorption dynamics, process optimization, and column operations for the removal and recovery of malachite green from wastewater using activated carbon and activated slag. *Ind. Eng. Chem. Res.* 36, 2207.
- Hall, K.R., Eagleton, L.C., Acrivos, A., Vermeulen, T., 1966. Pore solid diffusion kinetics in fixed bed adsorption under constant pattern conditions. *Ind. Eng. Chem. Fundam.* 5, 212.
- Hameed, B.H., El-Khaiary, M.I., 2008a. Batch removal of malachite green from aqueous solutions by adsorption on oil palm trunk fibre: equilibrium isotherms and kinetic studies. *J. Hazard. Mater.* 154, 237.
- Hameed, B.H., El-Khaiary, M.I., 2008b. Malachite green adsorption by rattan sawdust: isotherm, kinetic and mechanism modeling. *J. Hazard. Mater.* 159, 574.
- Hema, M., Arivoli, S., 2008. Adsorption kinetics and thermodynamics of malachite green dye onto acid activated low cost carbon. *J. Appl. Sci. Environ. Manage.* 12, 43.
- Ho, Y.S., McKay, G., 1998. Sorption of dye from aqueous solution by peat. *Chem. Eng. J.* 70, 115.
- Ho, Y.S., McKay, G., 1999. The sorption of lead(II) ions on peat. *Water Res.* 33 (2), 578.
- Kannan, N., Sundaram, M.M., 2001. Kinetics and mechanism of removal of methylene blue by adsorption on various carbons: a comparative study. *Dyes Pigm.* 1 (1), 25.
- Khan, A.A., Ahmad, R., Khan, A., Mondal, P.K., 2010. Preparation of unsaturated polyester Ce(IV) phosphate by plastic waste bottles and its application for removal of malachite green dye from water samples. *Arab. J. Chem.* <http://dx.doi.org/10.1016/j.arabjc.2010.10.012>.
- Khattari, S.D., Singh, M.K., 2009. Removal of malachite green from dye wastewater using neem sawdust by adsorption. *J. Hazard. Mater.* 167, 1089.
- Kumar, K.V., Ramamurthi, V., Sivanesan, S., 2006. Biosorption of malachite green, a cationic dye onto *Pithophora* sp., a fresh water algae. *Dyes Pigm.* 69, 102.
- Kumar, K.V., Sivanesan, S., 2007. Isotherms for malachite green onto rubber wood (*Hevea brasiliensis*) sawdust: comparison of linear and non-linear methods. *Dyes Pigm.* 72 (1), 124.
- Malik, R., Ramteke, D.S., Wate, S.R., 2007. Adsorption of malachite green on groundnut shell waste based powdered activated carbon. *Waste Manage.* 27, 1129.
- Mall, I.D., Srivastava, V.C., Agarwal, N.K., Mishra, I.M., 2005. Adsorptive removal of malachite green dye from aqueous solution by bagasse fly ash and activated carbon – kinetic study and equilibrium isotherm analyses. *Colloids Surf., A* 264 (1–3), 17.
- Mittal, A., 2006. Adsorption kinetics of removal of a toxic dye, malachite green, from wastewater by using hen feathers. *J. Hazard. Mater. B* 133, 196.
- Pan, X., Zhang, D., 2009. Removal of malachite green from water by *Firmiana* simplex wood fiber. *Electron. J. Biotechnol.* 12 (4), 1.
- Parimaladevi, P., Venkateswaran, V., 2011. Kinetics, thermodynamics and isotherm modeling of adsorption of triphenylmethane dyes (methyl violet, malachite green and magenta ii) on to fruit waste. *J. Appl. Technol. Environ. Sanit.* 1 (3), 273.
- Parthasarathy, S., Manjul, N., Hema, M., Arivoli, S., 2011. Removal of malachite green from industrial waste-water by activated carbon prepared from cashew nut bark Alfa Universal. *Int. J. Chem.* 2 (2), 41.
- Papinutti, L., Mouso, N., Forchiassin, F., 2006. Removal and degradation of the fungicide dye malachite green from aqueous solution using the system wheat bran–fomes sclerodermeus. *Enzyme Microb. Technol.* 39, 848.
- Saha, P., Chowdhury, S., Gupta, S., Kumar, I., Kumar, R., 2010. Assessment on the removal of malachite green using tamarind fruit shell as biosorbent. *Clean Soil Air Water* 38 (5–6), 437.
- Santhi, T., Manonmani, S., Smitha, T., 2010a. Removal of malachite green from aqueous solution by activated carbon prepared from the epicarp of *Ricinus communis* by adsorption. *J. Hazard. Mater.* 179, 178.
- Santhi, T., Manonmani, S., Smitha, T., 2010b. Kinetics and isotherm studies on cationic dyes adsorption onto *Annona squamosa* seed activated carbon. *Int. J. Eng. Sci. Technol.* 2 (3), 287.
- Santhi, T., Manonmani, S., Vasantha, V.S., Chang, Y.T., 2011. A new alternative adsorbent for the removal of cationic dyes from aqueous solution. *Arab. J. Chem.* <http://dx.doi.org/10.1016/j.arabjc.2011.06.004>.
- Sekhar, C.P., Kalidhasan, S., Rajesh, V., Rajesh, N., 2009. Biopolymer adsorbent for the removal of malachite green from aqueous solution. *Chemosphere* 77, 842.
- Srivastav, A.K., Srivastava, S.K., Srivastava, A.K., 1999. Response of serum calcium and inorganic phosphate of freshwater catfish, *Heteropneustes fossilis*, to chlorpyrifos. *Bull. Environ. Contam. Toxicol.* 58, 915.
- Srivastava, S., Sinha, R., Roy, D., 2004. Review: toxicological effects of malachite green. *Aquat. Toxicol.* 66, 319.
- Syed, S.P.S., 2011. Study of the removal of malachite green from aqueous solution by using solid agricultural waste. *Res. J. Chem. Sci.* 1 (1), 88.
- Tsai, W.T., Chen, H.R., 2010. Removal of malachite green from aqueous solution using low-cost chlorella-based biomass. *J. Hazard. Mater.* 175, 844.
- Yonar, M.E., Yonar, S.M., 2010. Changes in selected immunological parameters and antioxidant status of rainbow trout exposed to malachite green (*Oncorhynchus mykiss*, Walbaum, 1792). *Pestic. Biochem. Physiol.* 97 (1), 19.
- Zhang, J., Li, Y., Zhang, C., Jing, Y., 2008. Adsorption of malachite green from aqueous solution onto carbon prepared from *Arundo donax* root. *J. Hazard. Mater.* 50, 774.